

Linearly Single Polarization Fibers with Zero Polarization Mode Dispersion

KATSUNARI OKAMOTO, TOSHIHITO HOSAKA, AND YUTAKA SASAKI

Abstract—The optimum waveguide structure for linearly single polarization fibers, which satisfies the large modal birefringence and the zero polarization mode dispersion simultaneously, has been investigated. The basic waveguide structure is the single-mode optical fiber that has an elliptical core and stress-applying parts with a different expansion coefficient from that of the cladding. Waveguide parameters, such as index difference, core ellipticity, and cutoff wavelength, are first determined to obtain highly birefringent fibers with $B = 1 \times 10^{-5}$ or $B = 5 \times 10^{-5}$. The structure of the stress-applying parts that provides zero polarization mode dispersion is then determined.

I. INTRODUCTION

SINGLE-mode optical fibers that can maintain a state of polarization over a long length are desirable for use in coherent optical communications [1] and fiber-optic sensing systems [2]. Single-mode fibers capable of transmitting power in only one polarization state also have a great advantage in interconnecting single-mode fibers and polarization-sensitive devices such as integrated optical multiplexers and switches [3].

Two methods have been proposed to stabilize the state of polarization against environmental influences. One is to enhance the birefringence intentionally to reduce the coupling between the linearly polarized HE_{11}^x and HE_{11}^y modes [4]–[9]. The other is to twist the low-birefringence fiber to reduce the coupling between HE_{11}^+ mode (right-handed circularly polarized light) and HE_{11}^- mode (left-handed circularly polarized light) [10]. The former is called a linearly single polarization fiber. The latter is a circularly single polarization fiber.

For the linearly single polarization fiber, many papers concerning the fabrication technique and the polarization properties have been presented. Among them, the single polarization fibers reported by Hosaka *et al.* have modal birefringence $B = 8.5 \times 10^{-5}$ at $\lambda = 1.15 \mu\text{m}$, extinction ratio of 32 dB, and minimum loss of 0.53 dB/km at $\lambda = 1.58 \mu\text{m}$ [8], [11]. On the contrary, the polarization properties for the circularly single polarization fibers were examined using short lengths of fibers. Therefore, the polarization characteristics of long twisted fibers and the influence from external effects have not yet been clarified [12].

The major disadvantage for linearly single polarization fibers is that the polarization mode dispersion is fairly large. Polar-

ization mode dispersions for the elliptical core fibers or stress-induced birefringent fibers are of the order of 10–200 ps/km [13]–[15]. The residual cross-polarized component, which cannot be compensated for by the phase plate, arises from the polarization mode dispersion. This causes an adverse influence on the receiver sensitivity in the coherent optical communication systems [16] and the fiber-optic sensing systems. The concept of reducing polarization mode dispersion to zero was proposed by Tjaden [17] and Dyott *et al.* [18]. However, the contribution of the stress-induced birefringence was not considered in their analyses.

This paper presents the design of the optimum waveguide structure for linearly single polarization fibers that provides large modal birefringence, zero polarization mode dispersion, and low-loss properties simultaneously. Both geometrical anisotropy and stress-induced birefringence are taken into account in this paper, and on the basis of these analyses, the waveguide parameters such as index difference, core geometry, and stress-applying structures are determined.

II. LINEARLY SINGLE POLARIZATION FIBERS

The authors consider the basic waveguide structure as being the single-mode optical fiber that has stress-applying parts on both sides of the core [8] (Fig. 1). The following conditions must be satisfied simultaneously for the linearly single polarization fibers with zero polarization mode dispersion:

- 1) the modal birefringence should be large enough to maintain the input state of polarization,
- 2) the transmission loss should be as low as the ordinary circular symmetric fibers,
- 3) the polarization mode dispersion should be zero at the operating wavelength.

In Fig. 1 the stress-applying parts exert asymmetric stress to the core and cause strain birefringence in the core. When borosilicate glass is used in the stress-applying parts, the borosilicate glass must be separated from the core by more than five times the core radius in order to avoid loss increase due to B_2O_3 beyond $\lambda = 1.2 \mu\text{m}$ [19], [20]. Although the core may have an arbitrary shape, the authors will treat elliptical core fibers for convenience in the analysis of propagation characteristics. For the modal birefringence and polarization mode dispersion of the elliptical core fibers with small ellipticity, various methods of analysis have been presented by several authors [21]–[25]. However, transmission characteristics for elliptical core fibers with large ellipticity are not fully understood.

Manuscript received August 20, 1981; revised October 15, 1981.

The authors are with the Ibaraki Electrical Communication Laboratory, Nippon Telegraph and Telephone Public Corporation, Ibaraki-ken, Japan.

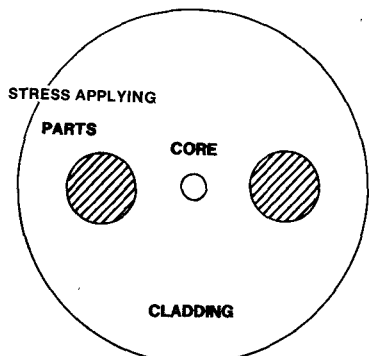


Fig. 1. Cross section of the linearly single polarization fiber.

A. Transmission Characteristics of Elliptical Core Fibers

Since the stress layer is separated from the core by more than five times the core radius, the influence of stress layer on the geometrical anisotropy can be ignored. Fig. 2 shows the geometry of the elliptical core fiber. The relative difference in refractive indexes between core and cladding Δ and the ellipticity of the core ϵ are defined as

$$\Delta = \frac{n_1^2 - n_2^2}{2n_1^2} \quad (1)$$

$$\epsilon = \frac{a - b}{a} \quad (2)$$

where n_1 is the refractive index of the core, n_2 is the refractive index of the cladding, and a and b are the semimajor and semiminor axes of the core, respectively. The two dominant modes of the elliptical core fibers are the HE_{11}^x (HE_{11}^{odd}) mode, in which the direction of the electric field vector lies along the major (x -coordinate) axis [Fig. 3(a)], and the HE_{11}^y (HE_{11}^{even}) mode, in which the electric field vector lies along the minor (y -coordinate) axis [Fig. 3(b)].

In calculating propagation constant, delay time, and waveguide dispersion, a numerical method was used based on the point-matching principle [26]. The point-matching method is a useful technique to analyze dispersion characteristics for homogeneous optical fibers with deformed core boundaries. The hybrid electromagnetic fields were expanded in terms of a linear combination of circular harmonics (Bessel's functions) and the boundary conditions are imposed on the fields at a finite number of points on the boundary. The propagation constant is given as the eigenvalue of the determinant equation whose elements are obtained by using Bessel's functions.

Figs. 4–6 show the normalized propagation constant, delay time, and waveguide dispersion as a function of normalized frequency v for elliptical core fibers with various ellipticities. In Figs. 4–6, the difference between HE_{11}^x and HE_{11}^y modes is too small to show in the figures. N_1 is a group index given by $N_1 = d(kn_1)/dk$, and normalized frequency v is defined as for the circular guide, using semimajor axis a as the equivalent radius, and is given by

$$v = kn_1 a \sqrt{2\Delta} \quad (3)$$

($k = 2\pi/\lambda$, λ is a wavelength of light in vacuum).

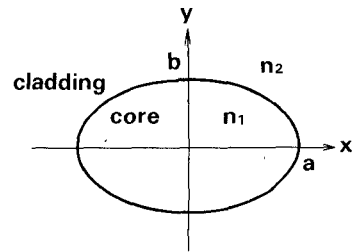


Fig. 2. Cross section of elliptical core.

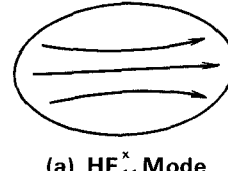
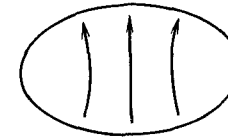
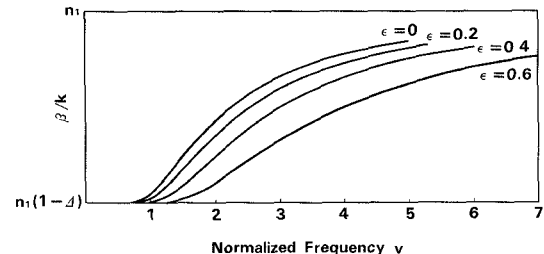
(a) HE_{11}^x Mode(b) HE_{11}^y ModeFig. 3. Field patterns for HE_{11}^x and HE_{11}^y modes.

Fig. 4. Normalized propagation constant for elliptical core fiber.

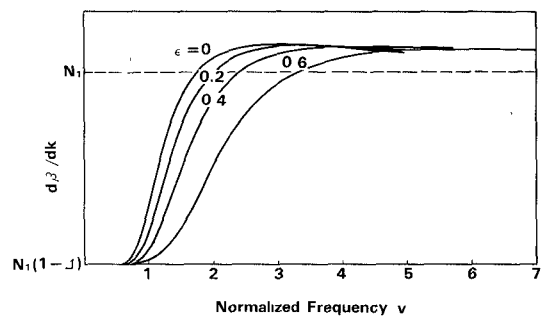


Fig. 5. Normalized delay time for elliptical core fiber.

The delay time per unit length τ and the waveguide dispersion ρ_w are obtained by

$$\tau = \frac{1}{c} \frac{d\beta}{dk} \quad (\text{ps/km}) \quad (4)$$

$$\rho_w = \frac{1}{c} \frac{1}{\lambda} k \frac{d^2 \beta}{dk^2} \quad (\text{ps/km/nm}) \quad (5)$$

where c is light velocity in vacuum.

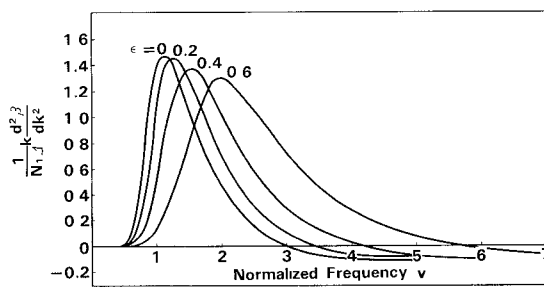


Fig. 6. Normalized waveguide dispersion for elliptical core fiber.

B. Modal Birefringence

When glass fiber with asymmetrical waveguide structure is subjected to stress, normalized propagation constants along the two principal stress directions are given by [27]

$$\beta_x/k = n_{x0} + C_1 \sigma_x + C_2 \sigma_y \quad (6)$$

$$\beta_y/k = n_{y0} + C_2 \sigma_x + C_1 \sigma_y \quad (7)$$

where C_1 and C_2 denote the stress-optical coefficients, and n_{x0} and n_{y0} are the effective refractive indexes of the fiber without asymmetrical stress which are defined as

$$n_{x0} = \beta_{x0}/k \quad (8)$$

$$n_{y0} = \beta_{y0}/k \quad (9)$$

where β_{x0} and β_{y0} denote the propagation constants for x and y polarizations, respectively. Then a modal birefringence is obtained from (6) and (7) by

$$B = \frac{\beta_x - \beta_y}{k} = B_g + B_s \quad (10)$$

$$B_g = (\beta_{x0} - \beta_{y0})/k \quad (11)$$

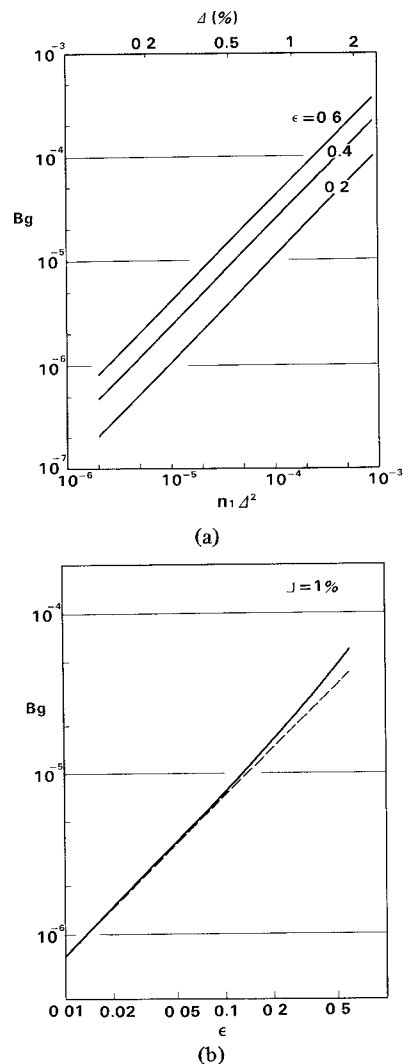
$$B_s = P \cdot (\sigma_x - \sigma_y) \quad (12)$$

where B_g denotes the geometrical anisotropy, B_s denotes the stress-induced birefringence, and P is the difference in stress-optical coefficients which is given as [28]

$$P = C_1 - C_2 = 3.36 \times 10^{-5} \text{ (mm}^2/\text{kg).} \quad (13)$$

It was shown in [17], [22], and [23] that the geometrical anisotropy of the elliptical core fibers with small ellipticity ($\epsilon \ll 1$) is proportional to $n_1 \Delta^2 \epsilon$. Then the relationship between geometrical anisotropy B_g and index difference Δ or ellipticity ϵ was first investigated. Fig. 7(a) shows the dependency of B_g on the square of index difference multiplied by the refractive index of the core $n_1 \Delta^2$. In Fig. 7(a), the maximum value of B_g is plotted for each ellipticity. That is, B_g at $v = 2.0$ for $\epsilon = 0.2$, $v = 2.4$ for $\epsilon = 0.4$, and $v = 3.0$ for $\epsilon = 0.6$ are illustrated. Fig. 7(a) shows that the geometrical anisotropy is proportional to $n_1 \Delta^2$. Fig. 7(b) shows the relationship between the geometrical anisotropy and the core ellipticity when the index difference is $\Delta = 1.0$ percent. The dotted line in Fig. 7(b) shows the line with inclination 45° . Therefore, it is shown from Fig. 7(b) that B_g is proportional to ellipticity when ϵ is much less than unity, and that B_g can be expressed as [29]

$$B_g = n_1 \Delta^2 [g_1(v) \epsilon + g_2(v) \epsilon^2 + \dots] \quad (14)$$

Fig. 7. (a) Variation of geometrical anisotropy B_g as a function of $n_1 \Delta^2$. (b) Variation of geometrical anisotropy B_g as a function of ϵ .

where g_1 and $g_2 \dots$ are functions of normalized frequency v . In this paper, the authors make use of the simple expression which is given by

$$B_g = n_1 \Delta^2 \epsilon G(v). \quad (15)$$

Since B_g is not proportional to ϵ for large ellipticities, the higher order correction terms in (14) are put into $G(v)$. The dependency of $G(v)$ on normalized frequency v is plotted in Fig. 8 for various ellipticities.

C. Polarization Mode Dispersion

The polarization mode dispersion for optical fibers with an asymmetrical waveguide structure is obtained by using (4) and (10)–(12) as

$$D = \tau_x - \tau_y = \frac{1}{c} \left(\frac{d\beta_x}{dk} - \frac{d\beta_y}{dk} \right) = \frac{1}{c} \left(\frac{d\beta_{x0}}{dk} - \frac{d\beta_{y0}}{dk} \right) + \frac{P}{c} \cdot (\sigma_x - \sigma_y). \quad (16)$$

In deriving (16), the authors used the property that the stress-optical coefficients are independent from wavelength [28]. The first term in (16) represents the polarization mode disper-

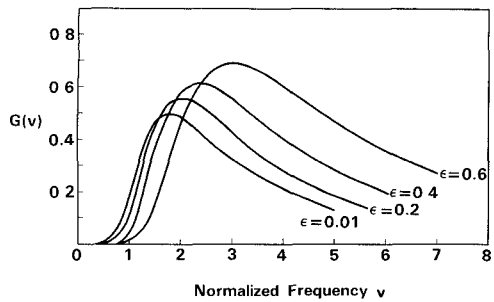


Fig. 8. Normalized phase constant difference $G(v)$ for various ellipticities.

sion due to asymmetrical core geometry (D_g) and the second represents that caused by asymmetrical stress (D_s). From (11), (15), and (16), D_g is given by

$$D_g = \frac{1}{c} \left(\frac{d\beta_{x0}}{dk} - \frac{d\beta_{y0}}{dk} \right) = \frac{1}{c} n_1 \Delta^2 \epsilon F(v) \quad (17)$$

where

$$F(v) = \frac{d}{dv} (vG). \quad (18)$$

Fig. 9 shows the dependency of $F(v)$ on normalized frequency v for various ellipticities.

Here, the difference in waveguide dispersions between the two polarization modes is noted. Substituting (16) into (5), the difference of waveguide dispersions is obtained as

$$\begin{aligned} \delta\rho_w &= \rho_{wx} - \rho_{wy} = \frac{1}{c} \frac{1}{\lambda} \left(k \frac{d^2\beta_x}{dk^2} - k \frac{d^2\beta_y}{dk^2} \right) \\ &= \frac{1}{c} \frac{1}{\lambda} \left(k \frac{d^2\beta_{x0}}{dk^2} - \frac{d^2\beta_{y0}}{dk^2} \right) = \frac{1}{c} \frac{1}{\lambda} n_1 \Delta^2 \epsilon S(v) \end{aligned} \quad (19)$$

where

$$S(v) = v \frac{dF}{dv}. \quad (20)$$

The dependency of $S(v)$ on normalized frequency v is shown in Fig. 10.

It is known from Fig. 10 that $S(v) = -1.65$ for the elliptical core fiber with $\epsilon = 0.2$, $\Delta = 1.0$ percent, and $v = 2.43$. Then the difference of waveguide dispersions at $\lambda = 1.3 \mu\text{m}$ is given from (19) as

$$\delta\rho_w = -0.07 \text{ (ps/km/nm)}. \quad (21)$$

Therefore, it is known that the difference in waveguide dispersions can be neglected in elliptical core fibers.

III. DESIGN OF THE ZERO POLARIZATION MODE DISPERSION FIBERS

A. Guiding Design Principle

From (16) and (17), the polarization mode dispersion for elliptical core fibers can be expressed as

$$D = \frac{1}{c} n_1 \Delta^2 \epsilon F(v) + \frac{P}{c} \cdot (\sigma_x - \sigma_y). \quad (22)$$

In order to make the polarization mode dispersion zero, the following condition must be satisfied:

$$n_1 \Delta^2 \epsilon F(v) + P \cdot (\sigma_x - \sigma_y) = 0. \quad (23)$$

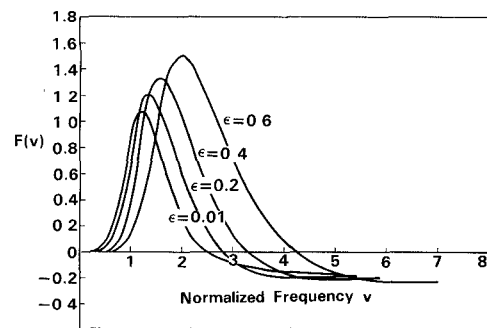


Fig. 9. Normalized delay time difference $F(v)$ for various ellipticities.

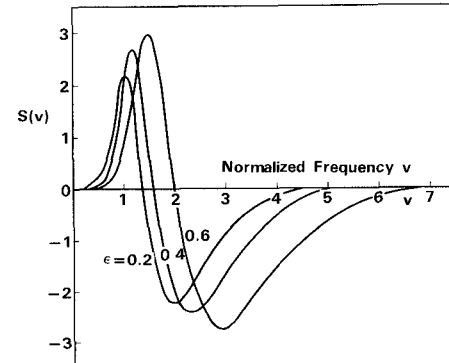


Fig. 10. Normalized waveguide dispersion difference $S(v)$ for various ellipticities.

When the above condition is met, modal birefringence B is expressed by using (10), (15), and (23) as

$$B = n_1 \Delta^2 \epsilon G(v) + P \cdot (\sigma_x - \sigma_y) = n_1 \Delta^2 \epsilon H(v) \quad (24)$$

where

$$H(v) = G(v) - F(v) = -v \frac{dG}{dv}. \quad (25)$$

$H(v)$ is plotted in Fig. 11 for various ellipticities.

Ulrich *et al.* have shown in their analysis on the bending-induced birefringence that the magnitude of modal birefringence due to bending becomes of the order of 1×10^{-6} when an optical fiber with outer diameter $2d = 125 \mu\text{m}$ is bent by bending radius $R = 1 \text{ cm}$ [30]. Therefore, in order to stabilize the state of polarization against the handling of optical fibers, modal birefringence of the fiber must be larger than about 1×10^{-5} . It was confirmed experimentally that in the linearly single polarization fibers made by the VAD method [31], modal birefringence $B = 1.5 \times 10^{-5}$ is sufficient to guarantee large extinction ratios between two polarizations.

In the design of waveguide structure, two cases, $B = 1 \times 10^{-5}$ (case 1) and $B = 5 \times 10^{-5}$ (case 2), will be treated. Therefore, the guiding design principle is as follows.

1) Determine waveguide parameters Δ , ϵ , and v so that the modal birefringence satisfies the condition $B = n_1 \Delta^2 \epsilon H(v) = 1 \times 10^{-5}$ or 5×10^{-5} , that is, $H(v) = 1 \times 10^{-5}/n_1 \Delta^2 \epsilon$ or $H(v) = 5 \times 10^{-5}/n_1 \Delta^2 \epsilon$. At this time, the value $n_1 \Delta^2 \epsilon F(v)$ is given by using the above waveguide parameters.

2) Determine the stress-applying structure so as to satisfy the condition $(\sigma_x - \sigma_y) = -n_1 \Delta^2 \epsilon F(v)/P$.

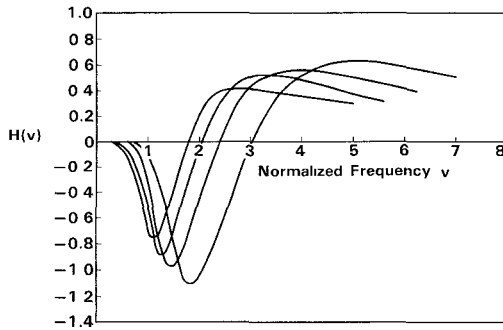


Fig. 11. Difference between normalized phase distortion and delay distortion $H(v) = G(v) - F(v)$ for various ellipticities.

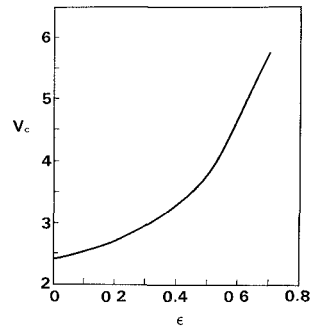


Fig. 12. Cutoff normalized frequency v_c for elliptical core fiber.

B. Design of the Waveguide Parameters

Before carrying out a concrete design of the waveguide parameters, cutoff normalized frequency v_c for elliptical core fibers was investigated. The relationship between v_c and ϵ is plotted in Fig. 12 [32]. The cutoff wavelength is given by

$$\lambda_c = \frac{2\pi}{v_c} n_1 a \sqrt{2\Delta}. \quad (26)$$

By combining (3) and (26), the ratio of the cutoff wavelength to the operating wavelength is given by

$$\frac{\lambda_c}{\lambda} = \frac{v}{v_c}. \quad (27)$$

Therefore, it is convenient to use the normalized ratio v/v_c as the operating parameter in describing the transmission properties of single-mode fibers. In Figs. 13-15, $G(v)$, $F(v)$, and $H(v)$ are plotted against ϵ by using v/v_c as an operating parameter.

It is necessary to determine waveguide parameters Δ , ϵ , and v/v_c so that the following conditions are satisfied:

$$H(v) = \frac{1 \times 10^{-5}}{n_1 \Delta^2 \epsilon} = Q_1(\Delta, \epsilon) \quad \text{for case 1} \quad (28)$$

and

$$H(v) = \frac{5 \times 10^{-5}}{n_1 \Delta^2 \epsilon} = Q_2(\Delta, \epsilon) \quad \text{for case 2.} \quad (29)$$

Q_1 and Q_2 are functions of index difference Δ and ellipticity ϵ , and are plotted in Figs. 16 and 17 against ϵ .

The combination of waveguide parameters Δ , ϵ , and v/v_c is given by the point at which $H(v)$ (Fig. 15) and Q_1 (Fig. 16) intersect for case 1 or the point at which $H(v)$ and Q_2 (Fig. 17)

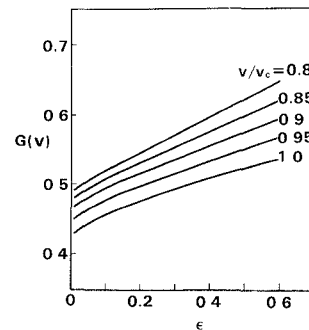


Fig. 13. Normalized phase constant difference as a function of ϵ .

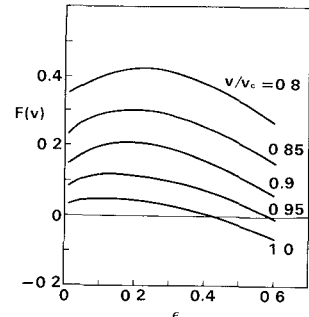


Fig. 14. Normalized delay difference as a function of ϵ .

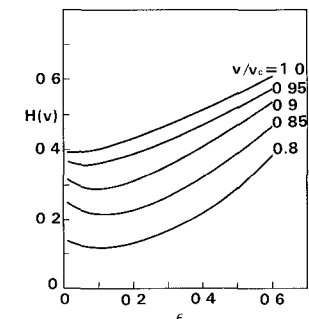


Fig. 15. Difference between normalized phase distortion and delay distortion $H(v) = G(v) - F(v)$ as a function of ϵ .

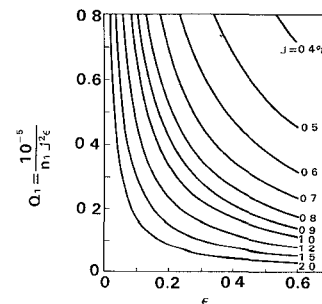
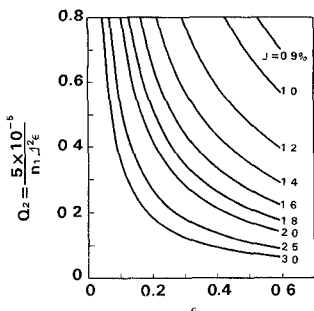
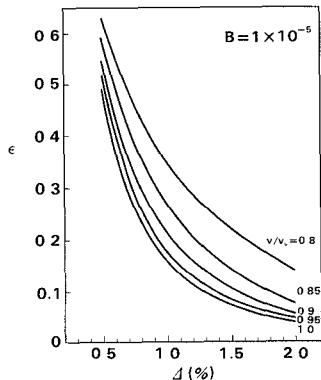
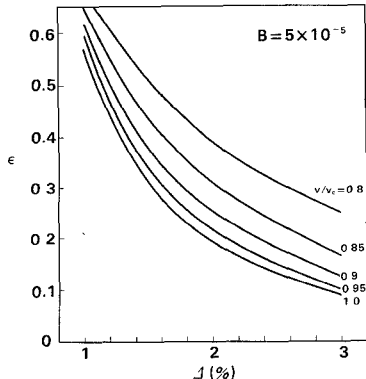


Fig. 16. Variation in $Q_1 = 1 \times 10^{-5}/n_1 \Delta^2 \epsilon$ as a function of ϵ .

intersect for case 2. The waveguide parameters thus obtained are shown in Fig. 18 (case 1) and Fig. 19 (case 2). It is known from Figs. 18 and 19 that index difference Δ must be greater than about 0.4 percent for $B = 1 \times 10^{-5}$ and $\Delta \geq 1.0$ percent for $B = 5 \times 10^{-5}$. It is possible to choose any waveguide parameters from Figs. 18 and 19 to obtain the zero polarization mode dispersion fibers.

Fig. 17. Variation in $Q_2 = 5 \times 10^{-5} / n_1 \Delta^2 \epsilon$ as a function of ϵ .Fig. 18. Waveguide parameters which give modal birefringence $B = n_1 \Delta^2 \epsilon H(v) = 1 \times 10^{-5}$ (Case 1).Fig. 19. Waveguide parameters which give modal birefringence $B = n_1 \Delta^2 \epsilon H(v) = 5 \times 10^{-5}$ (Case 2).

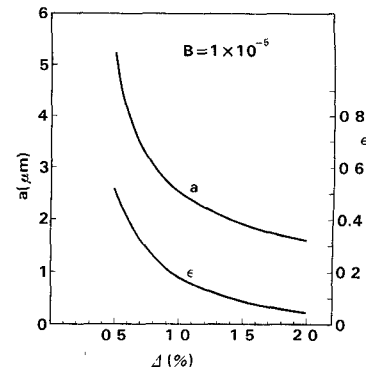
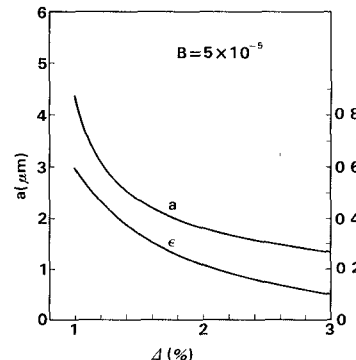
When operating parameter and wavelength are set to be $v/v_c = 0.95$ and $\lambda = 1.3 \mu\text{m}$ ($\lambda_c = 1.235 \mu\text{m}$), dependencies of core radius a and ellipticity ϵ on the index difference Δ are shown in Figs. 20 and 21.

C. Design of the Stress-Applying Structure

In the previous section, waveguide parameters to obtain the zero polarization mode dispersion have been determined. At the same time, the value $n_1 \Delta^2 \epsilon F(v)$ is also given by using the above waveguide parameters. Next, the stress-applying structure must be determined so as to satisfy the condition

$$\sigma_x - \sigma_y = -\frac{1}{P} n_1 \Delta^2 \epsilon F(v). \quad (30)$$

From Fig. 14, it is known that $F(v)$ is positive except for

Fig. 20. Core radius a and ellipticity ϵ as a function of Δ for operating parameter $v/v_c = 0.95$ (Case 1).Fig. 21. Core radius a and ellipticity ϵ as a function of Δ for operating parameter $v/v_c = 0.95$ (Case 2).

$v/v_c = 1.0$. Therefore, the stress difference in the core must satisfy the inequality as

$$\sigma_x - \sigma_y < 0. \quad (31)$$

It is known by stress analysis on elliptical core fibers [33] that the stress difference in the core is positive ($\sigma_x - \sigma_y > 0$) when there are no stress-applying parts. Then the stress-applying parts must be placed on both sides of the minor (y -coordinate) axis of the core (Fig. 22). In Fig. 22, one-quarter of the entire cross section is shown, and n_s denotes the refractive index of stress-applying part $2\theta_s$ which is the angle of stress part, and r_1 and r_2 are inner and outer radius of stress part, respectively. The diameter of the fiber is $2d = 125 \mu\text{m}$. The variation in stress difference in the core has been investigated when the molar concentration of dopant in the stress-applying part (borosilicate glass [34]) is increased. The relative index difference of the stress part Δ_s is defined by

$$\Delta_s = \frac{n_s^2 - n_2^2}{2n_2^2}. \quad (32)$$

The relationships between the stress difference and the index difference are shown in Figs. 23 and 24 for elliptical core fibers with $\Delta = 0.5$ percent, $\epsilon = 0.52$, and $a = 5.2 \mu\text{m}$ and $\Delta = 1.0$ percent, $\epsilon = 0.18$, and $a = 2.5 \mu\text{m}$, respectively.

In the calculation of stress difference, $r_1 = 5b$ and $r_2 = 10b$ were set and the finite element method [33] was used. It is shown from Figs. 23 and 24 that the stress difference ($\sigma_x - \sigma_y$) decreases and changes from positive to negative as the index difference (or molar concentration) of borosilicate glass becomes large.

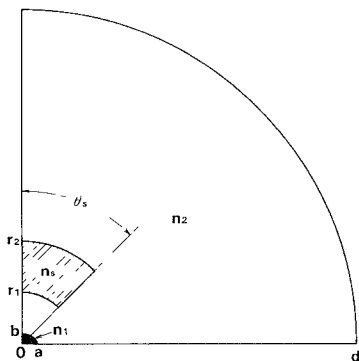
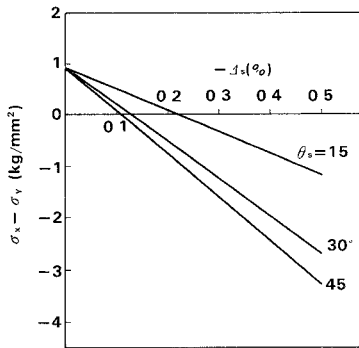
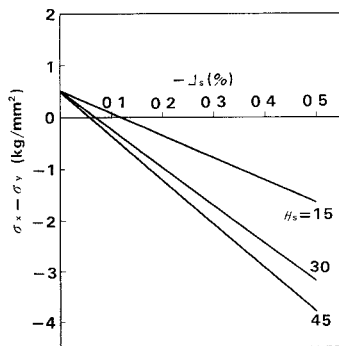


Fig. 22. Geometry of the stress-applying layer.

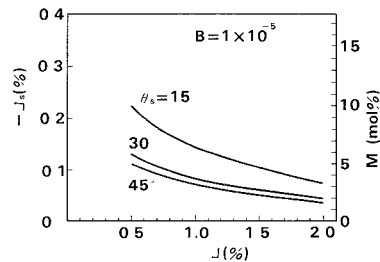
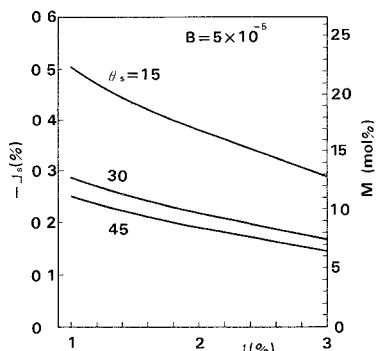
Fig. 23. Variation of stress difference in the core as a function of index difference $-\Delta_s$ of stress-applying layers for an elliptical core fiber with $\Delta = 0.5$ percent, $\epsilon = 0.52$, and $a = 5.2 \mu\text{m}$.Fig. 24. Variation of stress difference in the core as a function of index difference $-\Delta_s$ of stress-applying layers for an elliptical core fiber with $\Delta = 1.0$ percent, $\epsilon = 0.18$, and $a = 2.5 \mu\text{m}$.

On the basis of these results, the stress-applying structure was determined so as to satisfy the condition of (30). The calculated parameters for stress-applying parts are plotted in Fig. 25 (case 1) and Fig. 26 (case 2) against the index difference of the core.

To summarize the above investigations, the linearly single polarization fibers with zero polarization mode dispersion can be obtained by combination of waveguide parameters shown in Figs. 20 and 21 and the stress-applying structures shown in Figs. 25 and 26.

IV. CONCLUSIONS

An investigation has been made by numerical analysis on the optimum waveguide structure of linearly single polarization

Fig. 25. Refractive index difference $-\Delta_s$ for stress-applying layers to give zero polarization mode dispersion (Case 1).Fig. 26. Refractive index difference $-\Delta_s$ for stress-applying layers to give zero polarization mode dispersion (Case 2).

fibers which satisfies the zero polarization mode dispersion, large modal birefringence, and low-loss properties simultaneously. Waveguide parameters, such as the index difference in the core Δ , core ellipticity ϵ , and operating parameter v/v_c , are determined to obtain highly birefringent fibers with $B = 1 \times 10^{-5}$ or $B = 5 \times 10^{-5}$.

When borosilicate glass is used as the material of the stress-applying parts, it must be separated from the core by more than five times the core radius in order to prevent loss increase due to B_2O_3 beyond $\lambda = 1.2 \mu\text{m}$. Taking this into account, the structure of the stress-applying parts that provides zero polarization mode dispersion was determined. If there is no concern about the loss increase due to B_2O_3 or the light source in the $0.85 \mu\text{m}$ region is used, the side-pit fibers [7], in which the borosilicate parts are adjacent to the core, may also be a possible candidate for linearly single polarization fibers with zero polarization mode dispersion. However, the design of the waveguide structure for the side-pit fibers is very complicated because the existence of the borosilicate parts has influence on both geometrical anisotropy and stress-induced birefringence.

ACKNOWLEDGMENT

The authors would like to express their thanks to K. Matsuyama, H. Takata, and T. Manabe for their continuous encouragement and J. Noda and T. Edahiro for their fruitful discussion. They are also grateful to Prof. Yamashita of the University of Electro-Communication and K. Yamaguchi of Ibaraki ECL for kindly offering the computer program for the point-matching method.

REFERENCES

[1] T. Okoshi, "Heterodyne-type optical fiber communications," in *3rd IOOC, Tech. Dig. TUB1*, 1981, p. 44.

[2] R. Ulrich and M. Johnson, "Fiber-ring interferometer: Polarization analysis," *Opt. Lett.*, vol. 4, no. 5, pp. 152-154, 1979.

[3] R. A. Steinberg and T. G. Giallorenzi, "Performance limitation imposed on optical waveguide switches and modulator by polarization," *Appl. Opt.*, vol. 15, no. 10, pp. 2440-2453, 1976.

[4] V. Ramaswamy, I. P. Kaminow, and P. Kaiser, "Single polarization optical fibers: Exposed cladding technique," *Appl. Phys. Lett.*, vol. 33, no. 9, pp. 814-816, 1978.

[5] R. H. Stolen, V. Ramaswamy, P. Kaiser, and W. Pleibel, "Linear polarization in birefringent single-mode fibers," *Appl. Phys. Lett.*, vol. 33, no. 8, pp. 699-701, 1978.

[6] I. P. Kaminow, J. P. Simpson, H. M. Presby, and J. B. MacChesney, "Strain birefringence in single-polarization germanosilicate optical fibers," *Electron. Lett.*, vol. 15, no. 21, pp. 677-679, 1979.

[7] T. Hosaka, K. Okamoto, Y. Sasaki, and T. Edahiro, "Single-mode fibers with asymmetrical refractive-index pits on both sides of core," *Electron. Lett.*, vol. 17, no. 5, pp. 191-193, 1981.

[8] T. Hosaka, K. Okamoto, T. Miya, Y. Sasaki, and T. Edahiro, "Low-loss single polarization fibers with asymmetric strain birefringence," *Electron. Lett.*, vol. 17, no. 15, pp. 530-531, 1981.

[9] T. Katsuyama, H. Matsumura, and T. Suganuma, "Low-loss single-polarization fibers," *Electron. Lett.*, vol. 17, no. 13, pp. 473-474, 1981.

[10] L. Jeunhomme and M. Monerie, "Polarization-maintaining single-mode fiber cable design," *Electron. Lett.*, vol. 16, no. 24, pp. 921-922, 1980.

[11] T. Miya, Y. Sasaki, K. Okamoto, and T. Edahiro, "Polarization characteristics of several types of single-mode fibers," in *Proc. IECE Tech. Meet. on Opt. and Quantum Electron.*, Japan, vol. OQE81-59, 1981, pp. 49-54.

[12] A. J. Barlow and D. N. Payne, "Polarization maintenance in circularly birefringent fibers," *Electron. Lett.*, vol. 17, no. 11, pp. 388-389, 1981.

[13] S. C. Rashleigh and R. Ulrich, "Polarization mode dispersion in single-mode fibers," *Opt. Lett.*, vol. 3, no. 2, pp. 60-62, 1978.

[14] I. P. Kaminow, "Polarization in optical fibers," *IEEE J. Quantum Electron.*, vol. QE-17, pp. 15-22, Jan. 1981.

[15] N. Shibata, M. Tateda, S. Seikai, and N. Uchida, "Wavelength dependence of polarization mode dispersion in elliptical-core single-mode fibers," *Electron. Lett.*, vol. 17, no. 16, pp. 564-565, 1981.

[16] Y. Yamamoto and T. Kimura, "Coherent optical fiber transmission technology," in *Proc. IECE Tech. Meet. on Commun. Syst.*, Japan, vol. CS81-20, 1981, pp. 43-50.

[17] D. L. A. Tjaden, "Birefringence in single-mode optical fibers due to core ellipticity," *Philips J. Res.*, vol. 33, no. 5/6, pp. 254-263, 1978.

[18] R. B. Dyott, J. R. Cozens, and D. G. Morris, "Preservation of polarization in optical-fiber waveguides with elliptical cores," *Electron. Lett.*, vol. 15, no. 13, pp. 380-382, 1979.

[19] T. Izawa, N. Shibata, and A. Takeda, "Optical attenuation in pure and doped fused silica in ir wavelength region," *Appl. Phys. Lett.*, vol. 31, no. 1, pp. 33-35, 1977.

[20] H. Osanai, "Fabrication of ultra-low-loss low-OH-content high silica optical fiber," in *Electro-chem. Soc., Int. Fall Meet. Tech. Dig.*, 1978, p. 367.

[21] C. Yeh, "Elliptical dielectric waveguides," *J. Appl. Phys.*, vol. 33, no. 11, pp. 3235-3243, 1962.

[22] J. D. Love, R. A. Sammut, and A. W. Snyder, "Birefringence in elliptically deformed optical fibers," *Electron. Lett.*, vol. 15, no. 20, pp. 615-616, 1979.

[23] H. Tsuchiya and J. Sakai, "Characteristics of single-mode optical fiber with elliptical core," in *Proc. IECE Tech. Meet. on Opt. and Quantum Electron.*, Japan, vol. OQE74-86, 1974, pp. 21-30.

[24] Y. Fujii and K. Sano, "Polarization transmission characteristics of optical fibers with elliptical cross-section," *Trans. IECE Japan*, vol. J63-C, no. 8, pp. 471-477, 1980.

[25] C. Yeh, K. Ha, S. B. Dong, and W. P. Brown, "Single-mode optical waveguides," *Appl. Opt.*, vol. 18, no. 10, pp. 1490-1504, 1979.

[26] E. Yamashita, K. Atsuki, O. Hashimoto, and K. Kamijo, "Modal analysis of homogeneous optical fibers with deformed boundaries," *IEEE Trans. Microwave Theory Techn.*, vol. MTT-27, pp. 352-356, Apr. 1979.

[27] J. Tsuji, M. Nishida, and K. Kawada, "Experimental photoelasticity" (in Japanese), Nikkan Kogyo Co. Ltd.

[28] N. Imoto, N. Yoshizawa, J. Sakai, and H. Tsuchiya, "Birefringence in single-mode optical fiber due to elliptical core deformation and stress anisotropy," *IEEE J. Quantum Electron.*, vol. QE-16, pp. 1267-1271, Nov. 1980.

[29] R. A. Sammut, "Birefringence in slightly elliptical optical fibers," *Electron. Lett.*, vol. 16, no. 19, pp. 728-729, 1980.

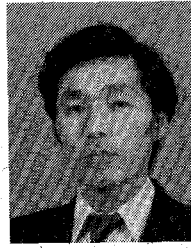
[30] R. Ulrich, S. C. Rashleigh, and W. Eickhoff, "Bending-induced birefringence in single-mode fibers," *Opt. Lett.*, vol. 5, no. 6, pp. 273-275, 1980.

[31] N. Niizeki, "Fabrication of low-loss and long-length optical fibers by VAD," in *Dig. Tech. Papers, 3rd IOOC*, 1981 p. 100.

[32] J. R. Cozens and R. B. Dyott, "Higher-mode cutoff in elliptical dielectric waveguides," *Electron. Lett.*, vol. 15, no. 18, pp. 558-559, 1979.

[33] K. Okamoto, T. Hosaka, and T. Edahiro, "Stress analysis of optical fibers by a finite element method," *IEEE J. Quantum Electron.*, vol. QE-17, pp. 2123-2129, Oct. 1981.

[34] S. E. Miller and A. G. Chynoweth, *Optical Fiber Telecommunications*. New York: Academic, 1979.



Katsunari Okamoto was born in Hiroshima Prefecture, Japan, on October 19, 1949. He received the B.S., M.S., and Ph.D. degrees in electronics engineering from Tokyo University, Tokyo, Japan, in 1972, 1974, and 1977, respectively.

He joined Ibaraki Electrical Communication Laboratory, N.T.T., Ibaraki-ken, Japan, in 1977, and has been engaged in research on the optimum waveguide structure of optical fibers.

Dr. Okamoto is a member of the Institute of Electronics and Communication Engineers of Japan.



Toshihito Hosaka was born in Yamanashi Prefecture, Japan, on June 18, 1953. He received the B.S. degree in electronics engineering from Yamanashi University, Yamanashi, Japan, in 1976.

He joined Ibaraki Electrical Communication Laboratory, N.T.T., Ibaraki-ken, Japan, in 1976, and has been engaged in research on fabrication of single-mode optical fibers.

Mr. Hosaka is a member of the Institute of Electronics and Communication Engineers of Japan.



Yutaka Sasaki was born in Niigata, Japan, on October 9, 1943. He received the B.S., M.S., and Ph.D. degrees, all in electronics engineering, from the Tokyo Institute of Technology, Tokyo, Japan, in 1967, 1969, and 1973, respectively.

He joined the Ibaraki Electrical Communication Laboratory, N.T.T., Ibaraki-ken, Japan, in 1973, and has been engaged in research on optical waveguides and optical devices such as thin film waveguides and Nd:YAG lasers.

Since 1980 he has been engaged in research on single polarization single-mode fibers and nonlinear effects in optical fibers.

Dr. Sasaki is a member of the Institute of Electronics and Communication Engineers of Japan and the Japan Society of Applied Physics.